J.Natn.Sci.Foundation Sri Lanka 2022 50 (2): 405 - 415
DOI: http://dx.doi.org/10.4038/jnsfsr.v50i2.10290

RESEARCH ARTICLE

Geotechnical engineering

Stability analysis of a partially saturated layered soil formation associated with shallow landslides

SC Walpita[1*], P Ratnaweera[2] and GWAR Fernando[3]

[1] *Department of Civil Engineering, Faculty of Engineering and Technology, CINEC Campus, Malabe, Sri Lanka.*
[2] *Department of Civil Engineering, Faculty of Engineering Technology, The Open University of Sri Lanka, Nawala, Nugegoda, Sri Lanka.*
[3] *Department of Physics, Faculty of Natural Sciences, The Open University of Sri Lanka, Nawala, Nugegoda, Sri Lanka.*

Submitted: 17 November 2020; Revised: 04 November 2021; Accepted: 24 December 2021

Abstract: In the event of a rainfall, the contrast in hydraulic conductivity and shear strength properties of a layered soil can be significant in determining the stability of a slope. The main objectives of this study were to model 1-D infiltration into a two-layered soil formation and to understand the effect of contrast in the permeability characteristics of the two layers on failure depth, time, and mechanism, in the event of a shallow landslide. Two hypothetical soils-relatively coarse and fine soils-were assumed for the layered soil model. 1-D infiltration into a partially saturated soil was modelled through the development of a finite difference numerical scheme by solving the mixed form of Richard's equation. The stability analysis has been conducted for varying rainfall intensities and permeabilities using a pre-defined stability envelope based on the pressure head. For the case where fine soil overlies the coarse soil in a two-layered model, results showed that the failure depth is significantly reduced when the saturated permeability of coarse soil decreases relative to the fine soil. The only possible failure mechanism was identified as 'loss of suction'. When the coarse soil overlain by a fine soil, no significant effect on failure depth has been observed. Both 'loss of suction' and the development of a 'perched water table' were identified as possible mechanisms. In both cases, it was noticed that the failure time decreases as the saturated permeability of coarse soil increases. The results suggest that contrast in permeability characteristics in layered soil formations plays a vital role in influencing failure time, depth, and mechanism.

Keywords: 1-D infiltration, layered soil, numerical solutions, partially saturated soil, pressure head, shallow landslides.

INTRODUCTION

In tropical countries such as Sri Lanka, landslides are predominantly activated by persistent, high-intensity rainfall. The customary type of landslides found in the central hill country of Sri Lanka are the flow slides, which are initiated by shallow rotational or translational slides (Cooray, 1994). The soil slopes in the hill areas, which are most susceptible to slides, mainly consist of residual soil and/or colluvium deposits. In general, tropical residual soils exhibit distinct soil layering due to the effect of weathering and tend to form more or less parallel to the ground surface (Huat *et al*., 2004). Layered soils may exhibit vertical contrast in hydraulic and shear strength properties as a result of the natural formation. In residual soils, the weathering process results in soil horizons from a particular parent source, which shows gradual or continuous vertical variations in hydraulic and mechanical properties (Rahardjo *et al.*, 2004).

In the event of a rainfall, the contrast in hydraulic conductivity and shear strength properties of layered soils can play a significant role in determining the stability of a slope. For instance, the presence of a highly conductive layer over a less conductive layer can cause a non-uniform pore water pressure profile, especially near the layer interface. Once the wetting front advances to the top of the less conductive layer, a rapid increase

[*] Corresponding author (walpita88@gmail.com; https://orcid.org/0000-0003-1387-4156)

in pore water pressure can be expected at the interface (Srivastava & Yeh, 1991). This may lead to a sudden decrease in shear resistance which results in failure. According to Blight (1997), if the residual soil mantle is relatively shallow in comparison to the length of the slope, a planar or a transitional slide may occur, and the stability of the soil mass with a planar failure surface should be analysed as an infinite slope.

The most common method to evaluate the stability of an infinite slope with a planar failure surface is based on the principle that the slope is stable if the magnitude of the shear strength (τ_f) exceeds its shear stress (τ). The shear strength, which is the maximum shear stress the slope could withstand without undergoing failure, can be determined based on the Mohr-Coulomb criterion:

$$\tau_f = c' + \sigma' tan\phi' \qquad ...(1)$$

Here, ϕ', c' and σ' are the effective angle of internal friction, effective cohesion, and the effective normal stress acting on the failure surface, respectively. Shear stress (τ) depends on several factors such as the unit weight of soil, pore water pressure and the slope angle. In general, the factor of safety, *F* can be defined as:

$$F = \frac{c' + \sigma' \cdot tan\phi'}{\tau} \qquad ...(2)$$

Skempton & Delory (1957) presented a simple method to determine the factor of safety, *F*, for an infinite planer sliding stratum with a depth *L* and slope angle *β* based on the Mohr-Coulomb failure criterion. This analysis considered the equilibrium of a soil strip element subjected to a constant water head of H. The factor of safety, *F* can be expressed as:

$$F = \frac{c' + (\gamma - \gamma_w H)\ L cos^2\beta \cdot tan\ \phi'}{\gamma L \cdot sin\beta \cdot cos\beta} \qquad ...(3)$$

Here, γ and γ_w represent the unit weight of soil and unit weight of water, respectively. Equation (3) can be used to determine *F* for a non-cohesive soil (*i.e.*, $c' = 0$) when the water table is at ground level (*i.e.*, $H = 1$) and when the soil is completely dry (*i.e.*, $H = 0$).

Stability analysis performed based on a completely dry or a completely saturated condition can be misleading since a partially saturated soil phase exists prior to saturation. Evaporation and evapo-transpiration cause a negative potential within the partially saturated soil matrix. This phenomenon leads to a negative pore water pressure or a matric suction. The theory of unsaturated soil mechanics explains that matric suction enhances soil shear strength. Matric suction, which is defined as the difference between pore-air and pore-water pressure (*i.e.*, $u_a - u_w$), increases the effective stress and can be expressed according to Bishop (1959), as:

$$\sigma' = \sigma - u_a + \chi(u_a - u_w) \qquad ...(4)$$

Here, χ is an effective stress parameter.

Fredlund *et al*. (1978) have expressed the Mohr-Coulomb failure envelope for partially saturated soils using two independent stress-state variables, σ′ and $(u_a - u_w)$ as:

$$\tau_f = c_t + \sigma' \cdot tan\phi' \qquad ...(5)$$

where, total cohesion, c_t is defined as $c_t = c' + (u_a - u_w) tan\phi^b$

The term ϕ^b represents the frictional resistance due to matric suction. Fredlund *et al.* (1996) proposed the shear strength equation of unsaturated soil shown in equation (6), where Θ is normalized volumetric water content, and R is an unknown fitting parameter used to determine the best-fit failure envelope with the experimental data.

$$\tau = c' + (\sigma_n - u_a)\ tan\phi' + (u_a - u_w)\ \Theta^R tan\phi' \qquad ...(6)$$

Equation (6) is a modification of equation (5), where the term ϕ^b is expressed as a function of Θ and ϕ'. Fredlund *et al*. (1996) suggested that $R = 1.0$ is a satisfactory prediction for a sandy soil, but *R* tends to increase with the plasticity of soils. To evaluate ϕ^b, the shear strength contributions due to effective cohesion $[c' + (u_a - u_w)\Theta^R tan\phi']$ can be plotted against matric suction. Plots between matric suction and shear strength at failure can be fitted based on three different approaches such as the linear envelope, second order polynomial, and that of Vanapalli *et al.* (1996). Kankanamge *et al*., (2018) conducted suction-monitored direct shear tests on compacted samples of residual soils in Sri Lanka (shear parameters c′ = 8.3 kPa & ϕ' = 32°), and determined a constant angle of ϕ^b = 11.8°. It was also shown that the linear envelope model could be used for the matric suctions ranging from 0 to 100 kPa.

When water infiltrates, the matric suction is gradually reduced, causing a reduction in the effective stress and hence the shear strength. Such a loss in shear strength may be sufficient to trigger certain shallow landslides (Fourie *et al*., 1999; Godt *et al*., 2009). The modified factor of safety, *F*, can be expressed as:

$$F = \frac{c' + (u_a - u_w)\tan\phi^b + (\gamma - \gamma_w H)\, L\cos^2\beta \tan\phi'}{\gamma\, L \sin\beta \cos\beta} \quad ...(7)$$

Even with these developments, the hydrological mechanisms causing failure in shallow slides are not yet completely understood (Meisina *et al.*, 2019). All failures cannot be attributed to one particular mechanism. Brönnimann (2011) postulates that failure mechanisms are predominantly due to an increase in the positive pore water pressure or due to loss of suction. The phenomenon of positive pore water pressure can be further classified into two types: a) due to the development of a perched water table when saturation occurs from the top of the stratum, and b) due to the upsurge of the groundwater table. Therefore, it is evident that the pressure head profile during the critical period of an infiltration event is paramount in determining the failure mechanism.

Collins and Znidarcic (2004) proposed a coupled formulation for an infinite slope analysis considering the effect of negative and positive pressure heads. This method pre-empts the time and critical depth of failure in relationship to the soil shear strength and rainfall parameters. Even though a soil slice can be treated as a one-dimensional soil column under rainwater infiltration, the effect of lateral seepage is also considered in this analysis to account for the slope angle. The formulation uses an approach which expresses the total forces acting on the part of the slice behind the wetting front as the sum of the effect of buoyant unit weight and seepage force. According to Collins and Znidarcic (2004), the stability equation can be given in the form of a critical depth of failure (d_{cr}), as shown in equation (8). Here h_c represent the negative pressure head which can be encountered in the unsaturated phase, while h_p stands for the positive pressure head, which develops after saturation. This equation indicates that for any pressure head value ranging from negative to positive, there exists a critical depth at which a failure could occur. If these conditions (pressure head value and respective depth) are satisfied for a particular slope during rainwater infiltration, failure can be expected. The application of this equation is further elaborated in the explanation associated with Figure 4.

$$d_{cr} = \frac{c' + \left(\gamma_w h_c \tan\phi^b - \gamma_w h_p \tan\phi'\right)}{\gamma\cos^2\beta\left(\tan\beta - \tan\phi'\right)} \quad ...(8)$$

As indicated in equations (7) and (8), rainwater infiltration in an unsaturated soil plays a vital role in determining the factor of safety of a particular slope. Therefore, it is imperative to gain an understanding of saturated and unsaturated flow through soil for an accurate assessment. Richards' equation (1931) is widely used to represent fluid flow through a partially saturated soil. This equation can be expressed in three different forms.

$$\frac{d\theta}{dh}\frac{\partial h}{\partial t} = \frac{\partial k}{\partial z}\frac{\partial h}{\partial z} + k\frac{\partial^2 h}{\partial z^2} - \frac{\partial k}{\partial z} \quad ...(9)$$

This is the pressure head based form, explained as above

$$\frac{\partial\theta}{\partial t} = \frac{\partial D}{\partial z}\frac{\partial\theta}{\partial z} + D\frac{\partial^2\theta}{\partial z^2} - \frac{\partial k}{\partial z} \quad ...(10)$$

This form expresses in terms of the volumetric water content based, as explained above.

$$\frac{\partial\theta}{\partial t} = \frac{\partial k}{\partial z}\frac{\partial h}{\partial z} + k\frac{\partial^2 h}{\partial z^2} - \frac{\partial k}{\partial z} \quad ...(11)$$

This is the mixed form, also explained as above. In equations 9, 10 and 11, t represents time, z is the spatial dimension, k is the unsaturated coefficient of permeability, θ is the volumetric water content, D is the unsaturated diffusivity, and h is the pressure head.

Due to the nonlinear nature of these equations, obtaining analytical solutions is not possible except for a few specific cases. In general, numerical techniques such as the Finite Difference Method and/or the Finite Element Method can be used to obtain a solution. Out of the three different forms of Richards' equation, the mixed form equation can be considered the most suitable for numerical modelling due to stability in numerical convergence and conservation of mass. Considering conservation of mass does not guarantee an accurate outcome since within an element of the FEM formulation, oscillatory solutions may be generated. This, however, does not occur in the finite difference formulation due to the diagonalization of the time matrix (Celia *et al.*, 1990).

The soil-water characteristic curve (SWCC) is a graphical illustration of the relationship that exists between the amount of water held within the soil pores and the applied matric suction (Fredlund, 2006). The accuracy of the SWCC enables accurate prediction of change in parameters θ and k with h, when used with Richards' equation. Figure 1 represents a typical SWCC with its significant parameters. The matric suction value at which air begins to displace the water in the largest pores of the soil mass is the air entry value. The residual volumetric water content θ_r represents the volumetric water content of a soil at which no further increase in suction causes a significant change in water content.

The saturated volumetric water content θ_s is indicative of the maximum water storage capacity of the soil. A relationship similar to Figure 1 can be observed for a plot between matric suction and the coefficient of permeability. Soil obtains its maximum value of the coefficient of permeability at saturation, and this tends to decrease as the matric suction increases.

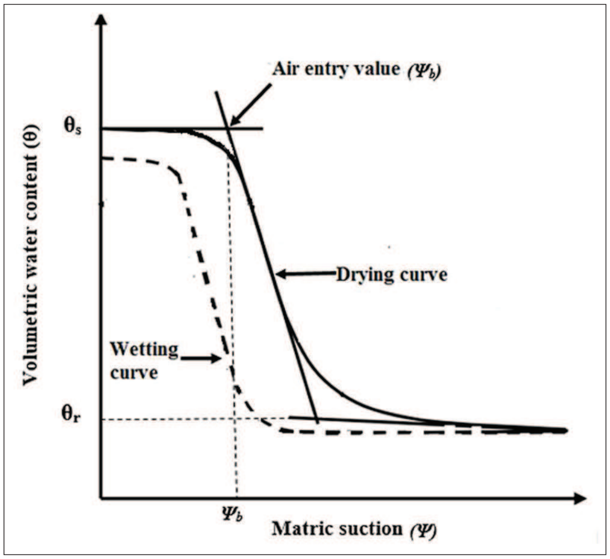

Figure 1: Typical soil water characteristic curve

Typical lab testing for the SWCC provides only a drying curve. The SWCC commonly reported in the literature is the drying curve rather than the wetting curve. This change in behaviour of the drying path and the wetting path is known as hysteresis. However, as the soil undergoes several wetting and drying cycles, this hysteresis effect becomes more and more insignificant. Natural soils have undergone numerous wetting and drying cycles, and therefore SWCC should be expected to fall within the two boundary curves.

According to Hillel (1998), the volumetric water content of a sandy soil decreases more sharply with the increasing matric suction compared to a clayey soil. Much greater steepness of the quasi-linear portion of the curve can be observed for a sandy soil when compared to a clayey soil. This is attributed to the difference in pore sizes and pore size distribution in the two soils. As defined by Fredlund *et al*. (1994), the air entry value is the matric suction value that must be exceeded before air recedes into the soil pores. The larger the air entry value, the higher the water retention ability at a given matric suction of a soil. In general, clayey soils exhibit greater air entry values compared to sandy soils.

According to the model proposed by Brooks and Corey (1964), the effective degree of saturation of a soil can be expressed as

$$S = \left(\frac{\psi_b}{\psi}\right)^{\lambda} \quad ...(12)$$

where λ is a shape parameter which expresses the steepness of the quasi-linear portion of the soil water characteristics curve. When the λ value gets smaller, the steepness of the curve tends to decrease. In principle, fine-grained soil possesses a smaller λ value compared to coarse-grained soil. With the inclusion of saturated permeability (k_s), the coefficient of permeability (k) of a given soil can be expressed, according to Brooks and Corey (1964), as

$$k = k_s^* S^{(3+\frac{2}{\lambda})} \quad ...(13)$$

Numerical solutions of modelled rainwater infiltration in unsaturated soils have been presented by researchers considering boundary conditions, the effect of multiple soil layers, different geometries, and varying rainfall conditions. For infinite slope analysis, the numerical solutions can be obtained using one-dimensional (1-D) infiltration. The 1-D model uses a soil column with vertical infiltration, which ignores the slope inclination and lateral seepage flow while taking the effect of ponding into account. When 1-D infiltration is to be adopted for an infinite slope analysis, the effect of ponding should be ignored due to the action of runoff. In a slope stability analysis, the 2-D model is capable of handling both slope inclination and lateral seepage flow, which is advantageous when special variability and soil inhomogeneity exist in the lateral direction. However, in the infinite slope theory, the soil is assumed to be homogeneous and isotropic, and therefore the 1-D model is adequate in analysing infinite slopes.

Many researchers have investigated slope instabilities using 1-D infiltration incorporated into an infinite slope model. Godt *et al.* (2012) conducted an infinite slope analysis for partially saturated soils using 1-D transient infiltration model and found that the depth and time of the potential slope failure depend on the soil water characteristics of the slope material. Zhan *et al.* (2013) analysed shallow slope failures in response to layered soil formations and concluded that slope angle, depth of least permeable layer, and rainfall intensity are significantly contribute to slope instability. According to the study conducted by Santoso *et al.* (2011) on a spatially variable slope in the depth direction, it was concluded that the failure probability values indicated by 1-D infiltration are much higher than those of 2-D analysis of the same slope. Also, it was observed that slope inclination and lateral flow have no significant impact on failure. By the equation (8) (as proposed by Collins and Znidarcic, 2004), the effect of lateral seepage force was also incorporated in the infinite slope analysis, which can be coupled with the 1-D infiltration analysis to obtain a critical failure depth of the slope.

In this particular study, the behaviour of 1-D infiltration into the simplest form of two-layered soil formation is being modelled, and attempts to understand the effect of contrast in the permeability characteristics of the two layers on failure depth, time, and mechanism.

MATERIALS AND METHODS

Stability model

In residual soil formations, different weathering grades and colluvium deposits may cause a layered soil profile with varying permeability characteristics. In order to understand the influence of varying permeability characteristics on failure mechanism, a hypothetical two-layered soil model was considered with the thickness of each layer set to 2m. The groundwater table was set at a depth of 4m from the ground surface. The saturated coefficient of permeabilities of the top layer and bottom layer were denoted as k_{s1} and k_{s2}, respectively. The following arrangements of two layers were considered using the two hypothetical soils, which exhibit coarse and fine characteristics.

i. Case A: fine soil overlain by the coarse soil ($k_{s1} < k_{s2}$)
ii. Case B: coarse soil overlain by the fine soil ($k_{s1} > k_{s2}$)

The above model was introduced with a varying rainfall intensity (I) at the top. Since the topsoil layer always controls the infiltration, the scenario of $I > k_{s1}$ was omitted, as the excess water will result in a runoff (no ponding). All the other possible scenarios, namely, $I = k_{s1} < k_{s2}$, $I < k_{s1} < k_{s2}$, $I < k_{s2} < k_{s1}$, and $k_{s2} < I < k_{s1}$, were analysed in this study.

Infiltration analysis

In a partially saturated soil, matric suction may cause permeability to be less than its saturated permeability. Richards' mixed form equation (11) for one-dimensional unsaturated flow (Richards, 1931) was used in this analysis to model the behaviour of infiltration. Therefore, a finite difference numerical scheme was developed by solving Richards' equation and programmed using MATLAB software.

By Euler's backward finite difference approximation, the discretized version of Richards' mixed form equation can be written as

$$\frac{\theta_j^{t+\Delta t} - \theta_j^t}{\Delta t} - \frac{k_{j+\frac{1}{2}}^{t+\Delta t} - k_{j-\frac{1}{2}}^{t+\Delta t}}{\Delta z} + \left[k_{j+\frac{1}{2}}^{t+\Delta t} * \frac{h_{j+1}^{t+\Delta t} - h_j^{t+\Delta t}}{\Delta z} - k_{j-\frac{1}{2}}^{t+\Delta t} * \frac{h_{j+1}^{t+\Delta t} - h_j^{t+\Delta t}}{\Delta z} \right] = 0 \quad ...(14)$$

Where, j is the spatial node at time stage t, Δz is the spatial discretization, Δt is the time step.

By introducing an iteration level '*m*' such as

$$h_j^{t+\Delta t,m+1} = h_j^{t+\Delta t,m} + \Delta h_j^{t+\Delta t,m+1} \quad ...(15)$$

The equation (14) can be rewritten as a tridiagonal system of linear equations

$$A*\Delta h_{j-1}^{t+\Delta t,m+1} + B*\Delta h_j^{t+\Delta t,m+1} + C*\Delta h_{j+1}^{t+\Delta t,m+1} = E \quad ...(16)$$

Here, *A*, *B*, *C*, and *E* are the respective coefficients of the linearized form after rearrangement. By solving the system of linear equations for $\Delta h_j^{t+\Delta t,m+1}$, the Picard iteration is set to continue until convergence is obtained for a pre-defined error (ε).

$$maximum \left| \boldsymbol{\Delta h_j^{t+\Delta t,m+1}} \right| < \varepsilon \quad ...(17)$$

Once the convergence criterion has been satisfied, the pressure head value is updated as shown in equation (15), before moving to the next time step.

Table 1 shows the Brooks and Corey parameters selected for the hypothetical soils (relatively coarse soil and fine soil). In terms of classification, the two soils can be approximated as a silty sand and a sandy silt, respectively. Figures 2 and 3 represent the permeability characteristics of the two soils.

Table 1: Assumed Brooks and Corey parameters for hypothetical soils

Fine soil	Coarse soil
θ_s = 0.45 (m^3/m^3)	θ_s = 0.35 (m^3/m^3)
θ_r = 0.20 (m^3/m^3)	θ_r = 0.05 (m^3/m^3)
λ = 0.2	λ = 0.5
Ψ_b= 1 kPa	Ψ_b = 10 kPa

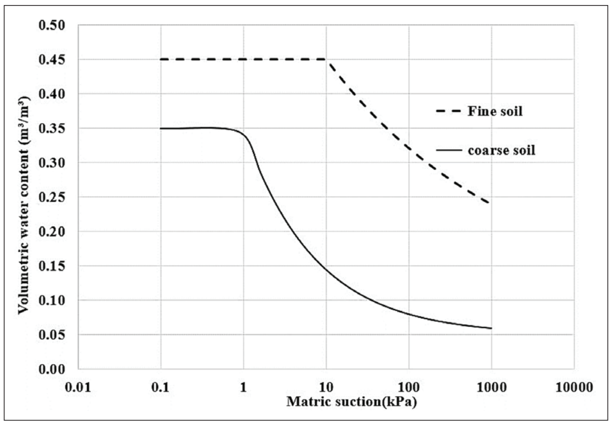

Figure 2: Soil water characteristic curves for hypothetical soils

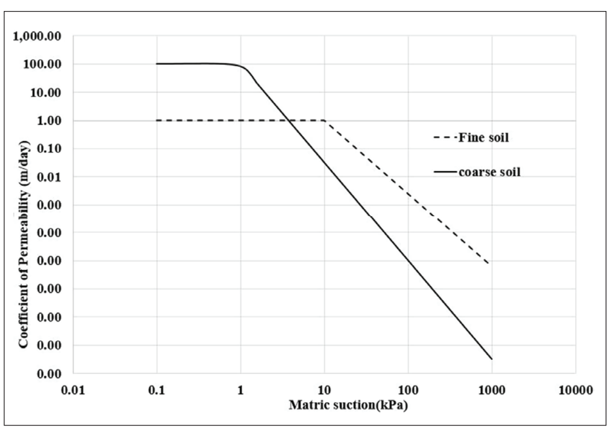

Figure 3: Coefficient of permeability curves for hypothetical soils when saturated permeability of fine soil is 1 m/day, and saturated permeability of coarse soil is 100 m/day

Stability analysis

The effective shear strength parameters for the two hypothetical soils were assumed as c' = 10 kPa and ϕ' = 20° for fine soil and c' = 3 kPa and ϕ' = 35° for coarse soil. The angle of frictional resistance due to matric suction (ϕ^b) has been determined using the linear envelope model, with the R value equal to one. For fine soil and coarse soil, it was calculated as 13.5° and 5°, respectively.

Throughout the analysis, the saturated permeability of fine soil was maintained at a constant value of 1 m/d, while different saturated permeability values were adopted for coarse soil. This analysis uses different permeability characteristics to represent the two layered formations and intends to study its effect on failure mechanism, failure depth and time.

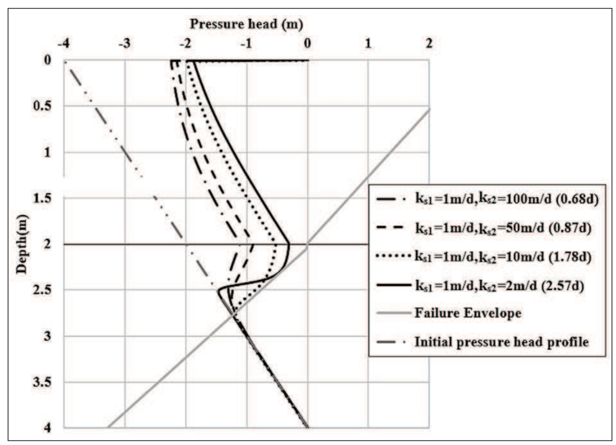

Figure 4: Stability analysis for case 1 (I = 0.1 m/day)

The failure envelope was generated based on Equation 8, with relevant shear strength parameters. Figure 4 shows the failure envelope generated for the case where the coarse soil is overlain by the fine soil. In principle, any given point on the failure envelope indicates the failure depth corresponding to its pressure head. It is seen that the failure envelope moves from a positive pressure head to a negative value, with increasing depth. This shows that slope failure could occur even under a negative pressure head condition, at higher depths and this is due to an increase in the effective weight of the sliding mass. Negative pressures at shallow depths do not trigger failure. Failure at shallow depths are associated with positive pressure conditions.

The initial pressure head profile shown in Figure 4 is based on the 'no infiltration' condition. This line represents zero hydraulic gradient and becomes a no-flow boundary condition. An infiltration-led pressure head profile can only be realized once the pressure head value at a given depth deviates from its initial boundary value. This interpretation indicates that the failure envelope plots towards the right-hand side of this no-flow boundary, which is within the zone of infiltration. The intersection between the failure envelope and the initial pressure head profile do not idealize a failure. Once infiltration takes place, the pressure head profile deviates from the initial boundary profile and intersects with the failure envelope, indicating a slope failure.

RESULTS AND DISCUSSION

Case A: $k_{s1} < k_{s2}$ (fine soil overlain by coarse soil)

When $I < k_{s1} < k_{s2,}$ (Figure 4), the development of positive pore water pressure of either of the soil layer cannot be expected since the rainfall intensity is not adequate to saturate either of the two soils. As a result, the pressure head profile always lie in the negative pressure head regime. To understand the infiltration process and its effect on the variation of the pressure head, it is important to refer to Figure 3, which illustrates the behaviour of the coefficient of permeability with negative pressure. As indicated in Figure 3, the coefficient of permeability of coarse soil remains quite low compared to fine soil for almost all the negative pressure values. For fine soil, the coefficient of permeability changes more gradually compared to coarse soil. Therefore, gradual reduction of matric suction or negative pressure can be observed throughout the infiltration process. However, when the wetting front reaches coarse soil, the water tends to percolate due to a smaller coefficient of permeability. Hence, the wetting front tends to move more slowly, and significant destruction of negative pressure takes place at lower wetting depth compared to fine soil. When the saturated permeability of coarse soil (k_{s2}) is reduced, this effect tends to be enhanced, and hence the pressure head profile moves abruptly rather than gradually towards the positive pressure regime. Therefore the failure point where the stability envelope meets the pressure head profile, becomes shallower and moves closer to the boundary between the two layers as the saturated permeability of coarse soil (k_{s2}) is reduced. The time taken for failure also tends to increase as k_{s2} reduces, and this phenomenon can be observed across all combinations belonging to case A (Table 3).

For the combination, $I = k_{s1} < k_{s2}$ (Figure 5), if the infiltration is continued, the development of positive pressure in the fine layer can be expected. However, due to the location of the stability envelope, which resides in a negative pressure regime, failure occurs before the saturation of the fine soil layer. Then again, the failure depth tends to decrease with decreased $k_{s2,}$ similar to Figure 4 but becomes more distinguishable due to the high rainfall intensity.

From the above observations, the loss of suction or negative pressure can be identified as the only possible failure mechanism pertinent to case A. It is also important to notice that the failure depth and failure

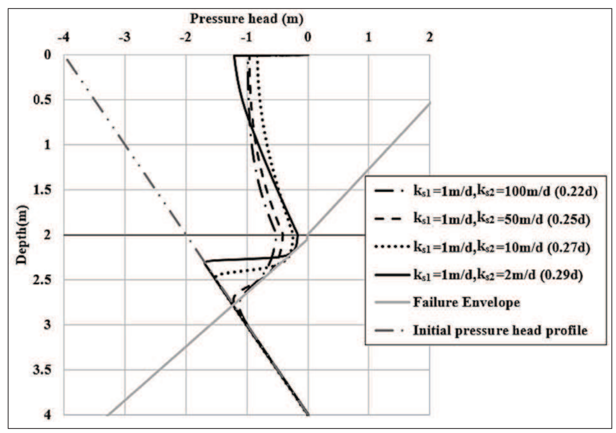

Figure 5: Stability analysis for case A (I = 1 m/day)

Table 2: Variation of failure depth with respect to different k_{s2} and I values

Saturated permeability of coarse soil (m/day)	Failure depth (m)		
	I = 0.1 m/day	I = 0.5 m/day	I = 1 m/day
100	2.75	2.75	2.73
50	2.75	2.74	2.46
10	2.74	2.31	2.27
2	2.31	2.28	2.15

time also tend to decrease when the k_{s1} approaches k_{s2} value. For instance, we can observe that the location at which the infiltration profile meets the failure envelope moves towards the boundary of the two layers as the k_{s2} value approaches k_{s1} (Figure 5). It is evident that the amount of water retained around the boundary and the active depth of infiltration depend upon the value of k_{s2}. When k_{s2} is less, more water will be retained around the boundary, which leads to steep destruction of negative pressure close to the boundary. Also, the active depth of infiltration in the bottom layer tends to be shallower due to the above fact. Therefore, the failure depth tends to decrease or move towards the boundary as the k_{s1} and k_{s2} values get closer. This particular trend has been consistently observed over different rainfall intensities, as shown in Table 2. These results indicate that if the difference in permeability values of the two layers is greater, an event of slope failure may move greater soil mass during a landslide and cause more damage.

As the k_{s2} value decreases, the time taken to destroy the negative pressure will increase and therefore, the time taken for failure also increases. Therefore, the further the k_{s2} value is away from k_{s1}, the shorter the time span after which failure may occur. In the event of a relatively shorter rainfall interval, it can be understood that the failure susceptibility increases with the difference in permeability values of the two layers. Similar to the failure depth, this observation has been consistently made over different rainfall intensities, as indicated in Table 3. Overall, it is fair to conclude that the larger the k_{s2} value, the more likely a slope is to fail quickly under any particular rainfall event.

As the rainfall intensity increases, it is observed that the aforementioned trends tend to continue with decreased failure depth and time (Tables 2 and 3). With increased intensity, destruction of negative pressure tends to take place closer to the boundary at a rapid pace due to the increased availability of water. It is important to notice that high-intensity rainfalls could cause failure in a shorter time period, while a persistent and relatively low-intensity rainfall may move a larger soil mass, which increases the magnitude of the damage.

Even though rainfall intensity such as 1 m/day is impractical to sustain throughout a day, it is important to notice that the failure occurs at a maximum of 0.29 days. The total rainfall received by the slope during this event until failure is around 290 mm. This is rare but definitely a possible high-intensity rainfall event that can be expected in the tropics.

Case B: $k_{s1} > k_{s2}$ (coarse soil overlain by fine soil)

Figure 6 elaborates the scenario pertaining to the combination $I < k_{s2} < k_{s1}$. Since the rainfall intensity is less than that of the saturated permeability of the coarse layer, saturation or development of positive pore water pressure cannot be expected. However, destruction of negative pressure takes place slowly at first and soon becomes a steady pressure head profile as the wetting front

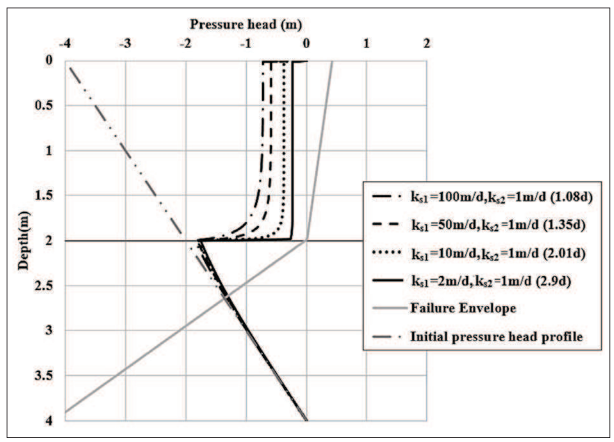

Figure 6: Stability analysis for case B (I = 0.1 m/day)

Table 3: Variation of failure time with respect to different k_{s2} and I values

Saturated permeability of coarse soil (m/day)	Failure time (days) I = 0.1 m/day	I = 0.5 m/day	I = 1 m/day
100	0.68	0.31	0.22
50	0.87	0.4	0.25
10	1.78	0.52	0.27
2	2.57	0.58	0.29

Table 4: Variation of failure depth with respect to different k_{s2} and I values (case B)

Saturated permeability of coarse soil (m/day)	Failure depth (m) I = 0.1 m/day	I = 0.5 m/day	I = 2 m/day
100	2.66	2.66	2.66
50	2.66	2.66	2.66
10	2.65	2.65	2.66
2	2.65	2.65	0.36

advances towards the boundary. Once the water reaches the fine layer, the wetting front tends to move quickly, with less resistance due to the higher permeability in the unsaturated phase. As a result, the wetting front advances relatively quickly and reduces the negative pressure so that the pressure head profile eventually meets the failure envelope. It is also observed that the failure depth tends to be almost the same for different values of k_{s1} (Table 4). Similar to case A, failure time tends to decrease as the saturated permeability of coarse soil (k_{s1}) is reduced, as shown in Table 5.

Table 5: Variation of failure time with respect to different k_{s2} and I values (case B)

Saturated permeability of coarse soil (m/day)	Failure time (days)		
	I = 0.1 m/day	I = 0.5 m/day	I = 2 m/day
100	1.08	0.32	0.12
50	1.35	0.39	0.13
10	2.01	0.55	0.18
2	2.9	0.8	0.19

The scenario $k_{s2} < I < k_{s1}$ is indicated by all the infiltration profiles (dashed curves), except the one shown as a solid curve in Figure 7. Similar to the previous scenario ($I < k_{s2} < k_{s1}$), failure depth tends to be almost constant. Since the saturated permeability of the top (coarse) layer is larger than that of rainfall intensity, no saturation will occur at the top layer. Positive pore water pressure is expected to build up at the boundary after a certain time since the saturated permeability of the bottom (fine) layer is lower than that of the rainfall intensity. If this occurs, failure at the boundary is a possibility. However, it can be seen (Figure 7) that failure occurs at the bottom layer before the occurrence of positive pore water pressure due to the small amount of water already seeping into the bottom layer.

The curve shown as a solid line in Figure 7 represents the scenario of $k_{s2} < I = k_{s1}$. The rainfall intensity is now equal to the saturated permeability value of coarse soil (top layer). Therefore, the amount of water seeping through the top layer will cause it to eventually become saturated. This results in a buildup of positive pore water or a perched water table at the top of the coarse soil layer. As the positive pressure increases, the pressure head profile eventually meets the failure envelope at a shallow depth and results in failure.

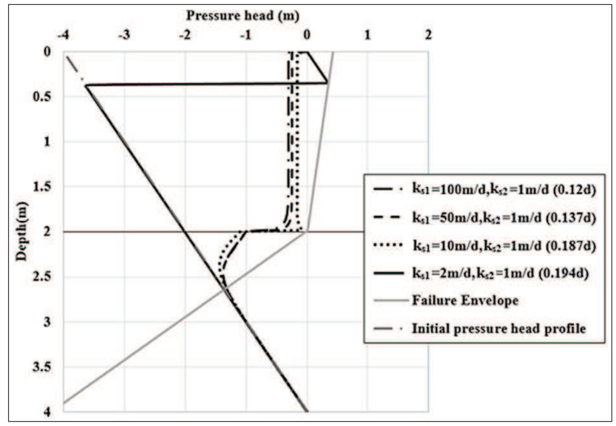

Figure 7: Stability analysis for case 2 (I = 2 m/day)

CONCLUSIONS

This study provides an insight to understand the planer failure occurring in shallow landslides, idealized considering a two-layered soil formation with varying permeability characteristics. It delivers several important observations on failure time, failure depth and the mechanism, under partially saturated conditions. Even though the saturated permeability of coarse soil is larger than the saturated hydraulic conductivity of fine soil, it is evident that the opposite behaviour takes place in the unsaturated phase and contributes significantly to the nature of the failure time and depth.

In the case where fine soil overlain by the coarse soil, a significant reduction of failure time and depth was observed as the saturated permeability of coarse soil increases relative to the fine soil. This has been consistently observed irrespective of the rainfall intensity. This phenomenon increases its susceptibility to failure under short rainfall events and, on the other hand, decreases the susceptibility to mobilize larger soil mass during failure. The only possible failure mechanism relevant to this particular case was identified as the 'loss of suction.'

In the case where coarse soil overlain by the fine soil, no significant trends or implications on failure depth have been observed in relation to the difference in saturated permeability between the two soils. Reduction of failure time has been observed as the saturated permeability of coarse soil increases relative to the fine soil. The failure mechanism is deemed more sensitive to the change in rainfall intensity. When the rainfall intensity is less than the saturated permeability of both soils, the failure occurs in the negative pore water pressure regime. Failure due to positive pore water pressure is only realized when the rainfall intensity exceeds the saturated permeability of the fine soil. Once the rainfall intensity exceeds the saturated permeability of the coarse soil, failure occurs due to the development of a perched water table.

This study concludes that contrasting permeability characteristics, the layer arrangement and the rainfall intensities of a two layer unsaturated soil formation tend to influence the failure time, depth, and the mechanism.

The model used in this study considers the layers to be homogeneous and the results are based on this idealization. The applicability of this study can be further enhanced by considering the influence of varying layer thickness on failure depth, failure time and the associated failure mechanism.

Acknowledgements

The authors gratefully acknowledge the support given by Mr. Ryan Haagenson and Professor Harihar Rajaram of University of Colorado. The MATLAB formulation used in this study is based on the initial work carried out by the said two researchers.

REFERENCES

Bishop A.W. (1959). The principle of effective stress. *Tecknisk Ukeblad* **106**(39): 859–863.

Blight G.E. (1997). Case histories of volume change and shear strength of residual soils. In: *Mechanics of Residual Soils* (eds. G.E. Blight & E.C. Leong), pp. 285–345. A.A. Balkema, Rotterdam, Netherlands.

Brönnimann C.S. (2011). Effect of groundwater on landslide triggering, *PhD Thesis*, Swiss Federal Institute of Technology, Lausanne, Switzerland.
DOI: https://doi.org/10.5075/epfl-thesis-5236

Brooks R. & Corey T. (1964). Hydraulic properties of porous media. *Hydrology Paper no 3*, Colorado State University, Colorado, USA. Available at *https://mountainscholar.org/bitstream/handle/10217/61288/HydrologyPapers_n3.pdf?/se*, Accessed 12 February 2019.

Celia M.A., Bouloutas E.T. & Zarba R.L. (1990). A general mass-conservative numerical solution for the unsaturated flow equation. *Water Resources Research* **26**(7): 1483–1496.
DOI: https://doi.org/10.1029/WR026i007p01483

Collins B.D. & Znidarcic D. (2004). Stability analyses of rainfall induced landslides. *Journal of Geotechnical and Geoenvironmental Engineering* **130**(4): 362–372.
DOI: https://doi.org/10.1061/(ASCE)1090-0241(2004)130:4(362)

Cooray P.G. (1994). Geological factors affecting landslides in Sri Lanka. *Proceedings of National Symposium of Landslides in Sri Lanka,* Colombo, Sri Lanka, pp. 15–22.

Fourie A.B., Rowe D. & Blight G.E. (1999). The effect of infiltration on the stability of the slopes of a dry ash dump. *Geotechnique* **49**(1): 1–13.
DOI: https://doi.org/10.1680/geot.1999.49.1.1

Fredlund D.G. (2006). Unsaturated soil mechanics in engineering practice. *Journal of Geotechnical and Geoenvironmental Engineering* **132**(3): 286–321.
DOI: https://doi.org/10.1061/(ASCE)1090-0241(2006)132:3(286)

Fredlund D.G., Morgenstern N.R. & Widger R.A. (1978). The shear strength of unsaturated soils. *Canadian Geotechnical Journal* **15**(3): 313–321.
DOI: https://doi.org/10.1139/t78-029

Fredlund D.G., Xing A. & Huang S. (1994). Predicting the permeability function for unsaturated soils using the soil-water characteristic curve. *Canadian Geotechnical Journal* **31**(4): 533–546.
DOI: https://doi.org/10.1139/t94-062

Fredlund D.G., Xing A., Fredlund M.D. & Barbour S.L. (1996). The relationship of the unsaturated soil shear strength to the soil-water characteristic curve. *Canadian Geotechnical Journal* **33**(3): 440–448.
DOI: https://doi.org/10.1139/t96-065

Godt J.W., Baum R.L. & Lu N. (2009). Landsliding in partially saturated materials. *Geophysical Research Letters* **36**(2): 1–5.
DOI: https://doi.org/10.1029/2008GL035996

Godt J.W., Şener-Kaya B., Lu N. & Baum R.L. (2012). Stability of infinite slopes under transient partially saturated seepage conditions. *Water Resources Research* **48**(5): 5505.

Hillel D. (1998). *Environmental Soil Physics: Fundamentals, Applications, and Environmental Considerations*. 1st edition, pp. 157–161. Academic Press, San Diego, USA.

Huat B.B., Gue S.S. & Ali F.H. (2004). *Tropical Residual Soils Engineering*, 1st edition, pp. 28–32. CRC Press, London, UK.

Kankanamge L., Jotisankasa A., Hunsachainan N. & Kulathilaka A. (2018.) Unsaturated shear strength of a Sri Lankan residual soil from a landslide-prone slope and its relationship with soil–water retention curve. *International Journal of Geosynthetics and Ground Engineering* **4**(3): 20–29.
DOI: https://doi.org/10.1007/s40891-018-0137-7

Meisina C., Bittelli M., Valentino R., Bordoni M. & Tomás-Jover R. (2019). Advances in shallow landslide hydrology and triggering mechanisms: a multidisciplinary approach. *Geofluids (Online)* 2019.
DOI: https://doi.org/10.1155/2019/1607684

Rahardjo H., Aung K.K., Leong E.C. & Rezaur R.B. (2004). Characteristics of residual soils in Singapore as formed by weathering. *Engineering Geology* **73**(1-2): 157–169.
DOI: https://doi.org/10.1016/j.enggeo.2004.01.002

Richards L.A. (1931). Capillary conduction of liquids through porous mediums. *Physics* **1**(5): 318–333.

Santoso A.M., Phoon K.K. & Quek S.T. (2011). Effects of soil

spatial variability on rainfall-induced landslides. *Computers and Structures* **89**(11–12): 893–900.
DOI: https://doi.org/10.1016/j.compstruc.2011.02.016

Skempton A.W. & DeLory F.A. (1957). Stability of natural slopes in London clay. *Proceedings of the Conference in Soil Mechanics,* London, UK, pp. 70–73.

Srivastava R. & Yeh T.C.J. (1991). Analytical solutions for one-dimensional, transient infiltration toward the water table in homogeneous and layered soils. *Water Resources Research* **27**(5): 753–762.
DOI: https://doi.org/10.1029/90WR02772

Vanapalli S.K., Fredlund D.G., Pufahl D.E. & Clifton A.W. (1996). Model for the prediction of shear strength with respect to soil suction. *Canadian Geotechnical Journal* **33**(3): 379–392
DOI: https://doi.org/10.1139/t96-060

Zhan T.L., Jia G.W., Chen Y.M., Fredlund D.G. & Li H. (2013). An analytical solution for rainfall infiltration into an unsaturated infinite slope and its application to slope stability analysis. *International Journal for Numerical and Analytical Methods in Geomechanics* **37**(12): 1737–1760.
DOI: https://doi.org/10.1002/nag.2106